INTERNATIONAL JOURNAL FOR NUMERICAL METHODS IN ENGINEERING
Int. J. Numer. Meth. Engng 2001; **50**:1759–1775

Modelling of elastic continua using a grillage of structural elements based on discrete element concepts

D. V. Griffiths*,†,§ and G. G. W. Mustoe‡

Colorado School of Mines, Golden, Colorado 80401-1887, U.S.A.

SUMMARY

A framework is described for modelling an elastic continuum using a grillage of beam-like structural elements derived from discrete element concepts. The beam element properties are derived in detail and implemented in a structural analysis code for validation against classical two-dimensional plane elasticity solutions. The framework offers the possibility of modelling the onset and propagation of fracture in materials that are initially continuous, without the need for specialized elements or remeshing in the context of traditional finite elements. Copyright © 2001 John Wiley & Sons, Ltd.

KEY WORDS: finite elements; continum modelling; discrete elements; elasticity; structural analysis; energy methods; numerical methods

INTRODUCTION

The numerical modelling of materials involving elastic-brittle behaviour is of considerable importance in several areas of engineering and applied science. The analysis of phenomena involving large-scale fracture is a complex problem requiring the development and application of sophisticated algorithms that can deal with mechanical contact, large rigid body motion and non-linear constitutive behaviour.

The idea of modelling an elastic continuum by a grillage of structural elements has been suggested by a number of workers, notably by Hrennikoff [1], and subsequently by researchers based in engineering and material science (e.g. References [2, 3]). Examples of discrete element method (DEM)-based algorithms for material failure include the rigid body-spring method developed by Kawai [4], Kawai *et al.* [5], and the simple deformable two- and three-dimensional polygonal discrete element procedures by Hocking *et al.* [6] and Mustoe [7].

More recently, a DEM employing a discretization of rigid circular particles connected together with linear normal and shear springs has been proposed by Morikawa *et al.* [8] and applied to

*Correspondence to: D. V. Griffiths, Division of Engineering, Colorado School of Mines, Golden, Colorado, 80401-1887, U.S.A
†E-mail: d.v.griffiths@mines.edu
§Professor
‡Associate Professor

Contract/grant sponsor: NSF; contract/grant numbers: CMS-9713442 and GER-9554559

Received 19 July 1999
Revised 19 April 2000

the dynamic analysis of fracture of reinforced concrete. This publication, together with an earlier work by Matsuoka *et al.* [9] contained only a brief description of the theoretical basis of their work and few validation examples.

The purpose of the current paper is to develop and validate this model for reproducing the static response of elastic solids using a grillage of structural elements based on discrete element concepts. The motivation for the work is the need to model materials which are initially solid and continuous, but eventually fracture and crack when critical stress and/or displacement levels are reached. The discrete element-based approach described herein offers the possibility of modelling such material behaviour within a consistent framework without the need for a switch in the analysis at the onset of fracture. Ultimately, the work is aimed at improving the scientific basis for understanding the mechanics of cutting technologies in civil and mining engineering as it applies to the excavation of geomaterials. The focus of the present paper however lies in the validation of the technique for modelling elastic continua.

STIFFNESS FORMULATION

The paper focuses on the use and validation of discrete elements to model the response of an elastic continuum subjected to various types of loading. The model is based on the work of Morikawa *et al.* [8] which considers a 2-D assembly of discrete cylindrical elements in a close pack hexagonal arrangement as shown in Figure 1. The discrete elements are touching each other and are attached at the point of tangency with normal and shear springs of stiffness k_n and k_s, respectively, as shown in Figure 2. It should be noted that for clarity, the figure shows the particles separated.

Consider two cylindrical discrete elements as shown in Figure 3. The local co-ordinate directions, x' and y', are oriented parallel and perpendicular respectively, to a line joining the centres of the particles. Each discrete element has three local degrees of freedom, a translation in the x'-direction, a translation in the y'-direction and a rotation (counterclockwise positive). The link with a more traditional finite element analysis is made by assuming that any two neighbouring discrete elements can be reduced to an equivalent two-node 'beam' finite element with three degrees of freedom per node. Each discrete element has a radius r which defines the length of the equivalent 'beam' element as $2r$.

Local beam element stiffness relationship

We now consider the symmetric stiffness relationship of the equivalent beam element in local co-ordinates. The standard stiffness relationship in matrix form can be written as

$$\mathbf{k}'\mathbf{u}' = \mathbf{f}' \tag{1}$$

where

$$\mathbf{k}' = \begin{bmatrix} k'_{11} & k'_{12} & k'_{13} & k'_{14} & k'_{15} & k'_{16} \\ k'_{21} & k'_{22} & k'_{23} & k'_{24} & k'_{25} & k'_{26} \\ k'_{31} & k'_{32} & k'_{33} & k'_{34} & k'_{35} & k'_{36} \\ k'_{41} & k'_{42} & k'_{43} & k'_{44} & k'_{45} & k'_{46} \\ k'_{51} & k'_{52} & k'_{53} & k'_{54} & k'_{55} & k'_{56} \\ k'_{61} & k'_{62} & k'_{63} & k'_{64} & k'_{65} & k'_{66} \end{bmatrix} \tag{2}$$

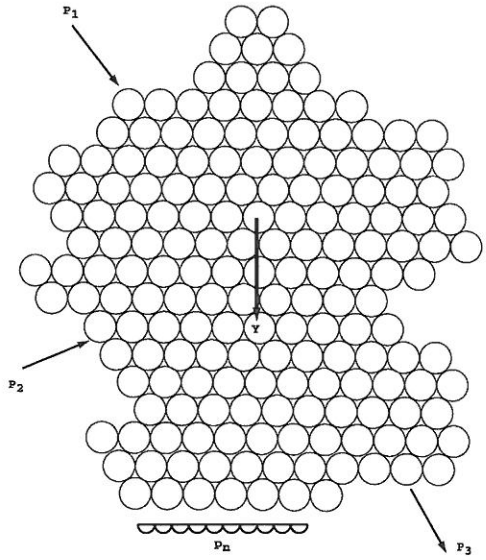

Figure 1. An assemblage of discrete elements subjected to various forces (P_1, etc), tractions (p_n) and body loads (Y).

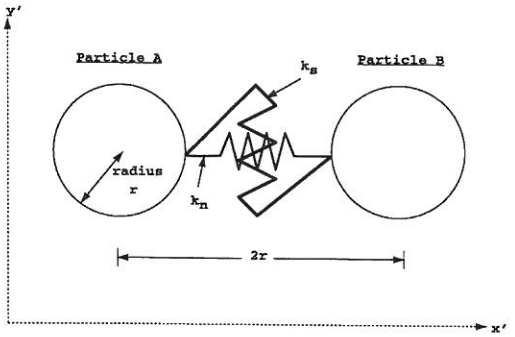

Figure 2. A two particle combination indicating the shear spring k_s and the normal spring k_n. The particles have been shown separated for clarity.

$$\mathbf{u}' = \begin{Bmatrix} u'_1 \\ u'_2 \\ u'_3 \\ u'_4 \\ u'_5 \\ u'_6 \end{Bmatrix} \tag{3}$$

and

$$\mathbf{f}' = \begin{Bmatrix} f'_1 \\ f'_2 \\ f'_3 \\ f'_4 \\ f'_5 \\ f'_6 \end{Bmatrix} \tag{4}$$

The $\mathbf{u}'$ vector holds the six element 'displacements' (translations and rotations) as shown in Figure 3, and the $\mathbf{f}'$ vector holds the six corresponding element 'loads' (forces and moments). For example, f'_1 would be a force applied in the x'-direction at node 1, f'_5 a force applied in the y'-direction at node 2, f'_6 a moment applied at node 2, and so on.

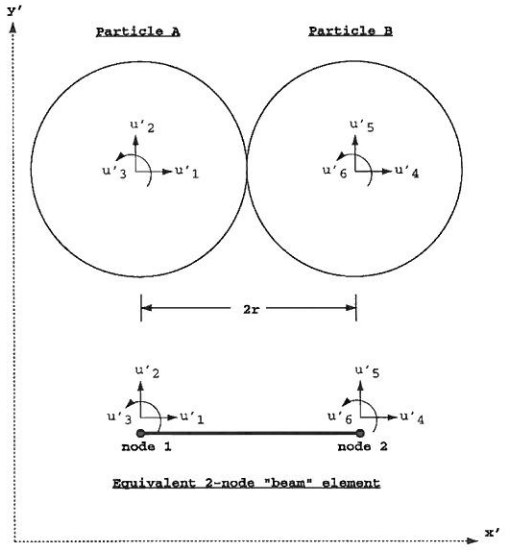

Figure 3. A two particle combination and its equivalent two-node 'beam' element counterpart. The element is aligned in the local x'-direction. (The springs are not drawn).

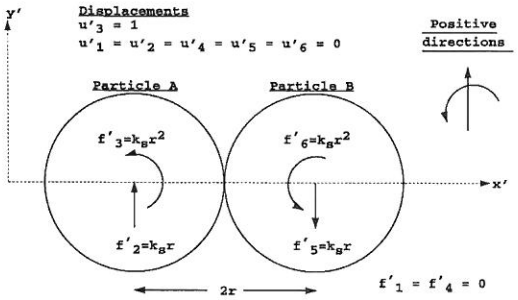

Figure 4. Forces required to maintain a unit rotation of particle A with all other displacements fixed to zero. These forces give the third column of the equivalent element stiffness matrix as shown in Equation (5). (The springs are not drawn).

To obtain the stiffness coefficients, *the unit displacement method* is used whereby we define k'_{ij} as the the force f'_i required to maintain the displacement pattern:

$$u'_k = \begin{cases} 1 & \text{if } k = j \\ 0 & \text{if } k \neq j \end{cases}$$

For example, the third column of $\mathbf{k}'$ holds the forces required to maintain the displacement field $u'_3 = 1$ (rotation) and $u'_1 = u'_2 = u'_4 = u'_5 = u'_6 = 0$ as shown in Figure 4. Each column of $\mathbf{k}'$ can therefore be completed by a simple equilibrium calculation of the forces required to hold each of the six unit displacement patterns. The resulting local element stiffness matrix is as follows:

$$\mathbf{k}' = \begin{bmatrix} k_n & 0 & 0 & -k_n & 0 & 0 \\ 0 & k_s & k_s r & 0 & -k_s & k_s r \\ 0 & k_s r & k_s r^2 & 0 & -k_s r & k_s r^2 \\ -k_n & 0 & 0 & k_n & 0 & 0 \\ 0 & -k_s & -k_s r & 0 & k_s & -k_s r \\ 0 & k_s r & k_s r^2 & 0 & -k_s r & k_s r^2 \end{bmatrix} \tag{5}$$

Global beam element stiffness relationship

In order to use the beam element in a general 2-D analysis, we need to consider the case where the line joining the centres of the two discrete elements is inclined to the global x-axis at an angle θ as shown in Figure 5. Each rotated element now has three global degrees of freedom at each node,

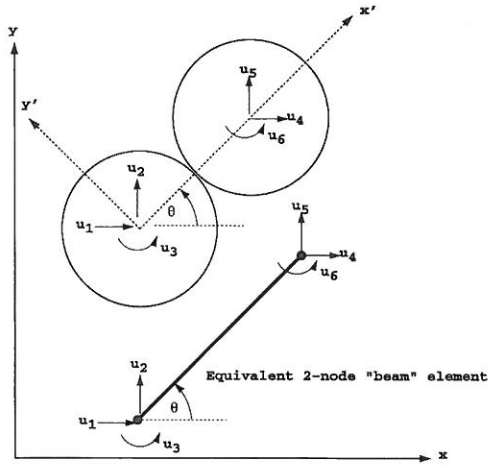

Figure 5. Two discrete elements rotated through an angle θ.

a translation in the x-direction, a translation in the y-direction and a rotation (counterclockwise positive).

The global stiffness relationship will now be given by

$$\mathbf{ku} = \mathbf{f} \tag{6}$$

where

$$\mathbf{k} = \begin{bmatrix} k_{11} & k_{12} & k_{13} & k_{14} & k_{15} & k_{16} \\ k_{21} & k_{22} & k_{23} & k_{24} & k_{25} & k_{26} \\ k_{31} & k_{32} & k_{33} & k_{34} & k_{35} & k_{36} \\ k_{41} & k_{42} & k_{43} & k_{44} & k_{45} & k_{46} \\ k_{51} & k_{52} & k_{53} & k_{54} & k_{55} & k_{56} \\ k_{61} & k_{62} & k_{63} & k_{64} & k_{65} & k_{66} \end{bmatrix} \tag{7}$$

$$\mathbf{u} = \begin{Bmatrix} u_1 \\ u_2 \\ u_3 \\ u_4 \\ u_5 \\ u_6 \end{Bmatrix} \tag{8}$$

and

$$\mathbf{f} = \begin{Bmatrix} f_1 \\ f_2 \\ f_3 \\ f_4 \\ f_5 \\ f_6 \end{Bmatrix} \tag{9}$$

Derivation of the global element stiffness matrix can be achieved by the use of a transformation matrix **t**. Consider the local element stiffness matrix $\mathbf{k}'$ partitioned into four quadrants, each in itself a 3×3 matrix as follows:

$$\mathbf{k}' = \begin{bmatrix} \mathbf{k}'_{11} & \mathbf{k}'_{12} \\ \mathbf{k}'_{21} & \mathbf{k}'_{22} \end{bmatrix} \tag{10}$$

Now, consider the transformation matrix

$$\mathbf{t} = \begin{bmatrix} c & s & 0 \\ -s & c & 0 \\ 0 & 0 & 1 \end{bmatrix} \tag{11}$$

where

$$c = \cos\theta \quad \text{and} \quad s = \sin\theta$$

The global stiffness matrix is then given by

$$\mathbf{k} = \begin{bmatrix} \mathbf{t}^{\mathrm{T}}\mathbf{k}'_{11}\mathbf{t} & \mathbf{t}^{\mathrm{T}}\mathbf{k}'_{12}\mathbf{t} \\ \mathbf{t}^{\mathrm{T}}\mathbf{k}'_{21}\mathbf{t} & \mathbf{t}^{\mathrm{T}}\mathbf{k}'_{22}\mathbf{t} \end{bmatrix} \tag{12}$$

which after expansion leads to

$$\mathbf{k} = \begin{bmatrix} k_{\mathrm{n}}c^2 + k_{\mathrm{s}}s^2 & (k_{\mathrm{n}} - k_{\mathrm{s}})sc & -k_{\mathrm{s}}rs & -(k_{\mathrm{n}}c^2 + k_{\mathrm{s}}s^2) & -(k_{\mathrm{n}} - k_{\mathrm{s}})sc & -k_{\mathrm{s}}rs \\ & k_{\mathrm{n}}s^2 + k_{\mathrm{s}}c^2 & k_{\mathrm{s}}rc & -(k_{\mathrm{n}} - k_{\mathrm{s}})sc & -(k_{\mathrm{n}}s^2 + k_{\mathrm{s}}c^2) & k_{\mathrm{s}}rc \\ & & k_{\mathrm{s}}r^2 & k_{\mathrm{s}}rs & -k_{\mathrm{s}}rc & k_{\mathrm{s}}r^2 \\ & & & k_{\mathrm{n}}c^2 + k_{\mathrm{s}}s^2 & (k_{\mathrm{n}} - k_{\mathrm{s}})sc & k_{\mathrm{s}}rs \\ & & & & k_{\mathrm{n}}s^2 + k_{\mathrm{s}}c^2 & -k_{\mathrm{s}}rc \\ & & & & & k_{\mathrm{s}}r^2 \end{bmatrix} \tag{13}$$

Note that the **k** matrix is symmetric so only the upper triangular terms have been included for clarity. Note also that the transformation has no effect on the rotations or moments, thus $u'_3 = u_3$, $u'_6 = u_6$, $f'_3 = f_3$ and $f'_6 = f_6$.

RELATIONSHIP WITH SOLID ELASTICITY

In order to develop a relationship between the spring stiffnesses k_{s} and k_{n} and the solid elasticity parameters E and ν we consider a small region of material as shown in Figure 6. The figure shows three cylinders in a close-packed hexagonal arrangement. The resulting equilateral triangle described by the 'beam' elements attached to the centre of each element will be considered a basic unit of material in the formulation.

The derivation makes use of the strain energy density V_0 of a deformed elastic body which has the property (see e.g. Reference [10]) that its derivative with respect to any strain component

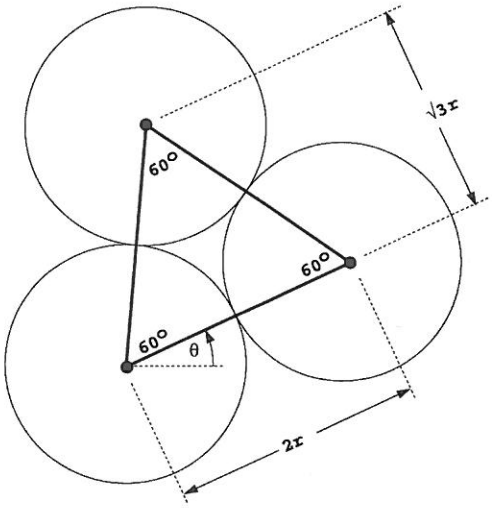

Figure 6. Three elements modelling a small region of elastic material. This arrangement represents a basic unit of material.

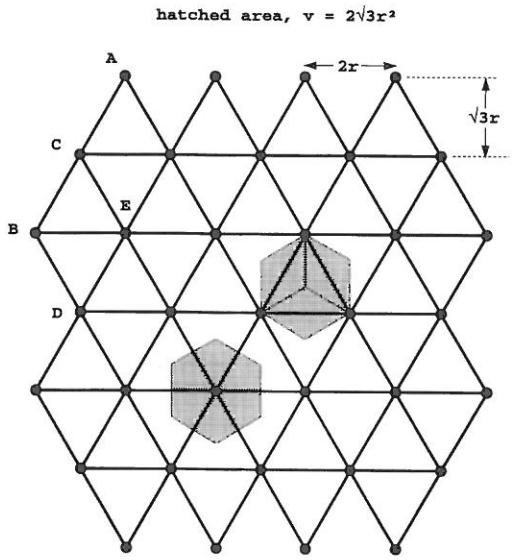

Figure 7. Zone of influence of a typical node or a typical equilateral arrangement. In both cases the hatched area is twice the equilateral area.

gives the corresponding stress component, for example:

$$\frac{\partial V_o}{\partial \varepsilon_{xx}} = \sigma_{xx}$$

$$\frac{\partial V_o}{\partial \varepsilon_{yy}} = \sigma_{yy}$$

$$\frac{\partial V_o}{\partial \varepsilon_{xy}} = \sigma_{xy} \tag{14}$$

$$\frac{\partial V_o}{\partial \varepsilon_{yx}} = \sigma_{yx}$$

Strain energy stored

The first step is to derive the strain energy stored in the unit of material shown in Figure 6 when it is subjected to an arbitrary nodal displacements. Initially we consider a single element as defined by two cylinders oriented along the local x'-axis as shown in Figure 2. The energy stored is given by

$$W = \frac{1}{2}\sum_{i=1}^{6} f_i u_i \tag{15}$$

which from Equation (1) can be written in matrix form as

$$W = \tfrac{1}{2}(\mathbf{u}')^{\mathrm{T}}\mathbf{f}' = \tfrac{1}{2}(\mathbf{u}')^{\mathrm{T}}\mathbf{k}'\mathbf{u}' \tag{16}$$

Expansion of Equation (16) leads to

$$W = \frac{k_{\mathrm{n}}}{2}(u_4' - u_1')^2 + \frac{k_{\mathrm{s}}}{2}(u_5' - u_2' - 2r\beta)^2 \tag{17}$$

where the average rotation

$$\beta = \frac{u_3' + u_6'}{2}$$

In terms of nodal displacements, the axial strain and rotation of the local element ($\theta = 0$) are given by

$$\varepsilon_\theta = \frac{u_4' - u_1'}{2r}$$

and

$$\psi_\theta = \frac{u_5' - u_2'}{2r}$$

thus Equation (17) can be written in the form

$$W(\theta) = 2r^2 k_{\mathrm{n}}\varepsilon_\theta^2 + 2r^2 k_{\mathrm{s}}(\psi_\theta - \beta)^2 \tag{18}$$

For a general element oriented at θ to the horizontal as shown in Figure 5, the axial strain and rotation of the element can be expressed in terms of global strain quantities [10] through the transformation equations:

$$\varepsilon_\theta = c^2\varepsilon_{xx} + sc(\varepsilon_{xy} + \varepsilon_{yx}) + s^2\varepsilon_{yy} \tag{19}$$

$$\psi_\theta = c^2\varepsilon_{yx} + sc(\varepsilon_{yy} - \varepsilon_{xx}) - s^2\varepsilon_{xy} \tag{20}$$

Substitution of Equations (19) and (20) into (18), gives the energy stored in a general element oriented at θ to the horizontal as

$$W(\theta) = 2r^2 k_{\mathrm{n}}(c^2\varepsilon_{xx} + sc(\varepsilon_{xy} + \varepsilon_{yx}) + s^2\varepsilon_{yy})^2 + 2r^2 k_{\mathrm{s}}(c^2\varepsilon_{yx} + sc(\varepsilon_{yy} - \varepsilon_{xx}) - s^2\varepsilon_{xy} - \beta)^2 \tag{21}$$

For a general equilateral triangular linkage of three elements, such as shown in Figure 6, the total energy stored is given by

$$W_{\mathrm{tot}} = W(\theta) + W(\theta + \pi/3) + W(\theta + 2\pi/3) \tag{22}$$

leading to the following expression which is invariant with respect to the angle θ:

$$\begin{aligned} W_{\mathrm{tot}} = {} & 3r^2(3k_{\mathrm{n}} + k_{\mathrm{s}})(\varepsilon_{xx}^2 + \varepsilon_{yy}^2)/4 + 3r^2(k_{\mathrm{n}} - k_{\mathrm{s}})(\varepsilon_{xx}\varepsilon_{yy} + \varepsilon_{xy}\varepsilon_{yx})/2 \\ & + 3r^2(k_{\mathrm{n}} + 3k_{\mathrm{s}})(\varepsilon_{xy}^2 + \varepsilon_{yx}^2)/4 + 6r^2\beta k_{\mathrm{s}}(\varepsilon_{xy} - \varepsilon_{yx}) + 6r^2\beta^2 k_{\mathrm{s}} \end{aligned} \tag{23}$$

Strain energy density

In order to compute the strain energy density V_o, a nominal 'volume' v must be assigned to each equilateral arrangement. From Figure 7, and assuming planar conditions, it is shown that any element connecting two nodes represents one third of the equilateral region to each side. This implies that the zone of influence of any internal triangular arrangement of elements covers six-thirds or twice the enclosed area. An alternative interpretation is to consider the zone of influence of each node (or discrete element) which also leads to a volume given by

$$v = 2\sqrt{3}r^2 \tag{24}$$

Evaluating the strain energy density as

$$V_o = W_{tot}/v \tag{25}$$

and differentiating with respect to each of the strain terms as shown in Equations (14) leads to

$$\begin{aligned}
\frac{\partial V_o}{\partial \varepsilon_{xx}} &= \sigma_{xx} = \frac{\sqrt{3}}{4}(3k_n + k_s)\varepsilon_{xx} + \frac{\sqrt{3}}{4}(k_n - k_s)\varepsilon_{yy} \\
\frac{\partial V_o}{\partial \varepsilon_{yy}} &= \sigma_{yy} = \frac{\sqrt{3}}{4}(k_n - k_s)\varepsilon_{xx} + \frac{\sqrt{3}}{4}(3k_n + k_s)\varepsilon_{yy} \\
\frac{1}{2}\left(\frac{\partial V_o}{\partial \varepsilon_{xy}} + \frac{\partial V_o}{\partial \varepsilon_{yx}}\right) &= \tau_{xy} = \frac{\sqrt{3}}{4}(k_n + k_s)\gamma_{xy}
\end{aligned} \tag{26}$$

It will be noted that the conventional shear stress τ_{xy} and 'engineer's' shear strain measures have been introduced at this point where:

$$\tau_{xy} = \tfrac{1}{2}(\sigma_{xy} + \sigma_{yx})$$

and

$$\gamma_{xy} = \varepsilon_{xy} + \varepsilon_{yx}$$

Relationship with plane strain and plane stress

Equations (26) enable a direct comparison to be made between this discrete element formulation and classical 2-D plane elasticity in terms of Young's Modulus and Poisson's Ratio. The equivalent expressions are given by

Plane strain:

$$\begin{aligned}
\sigma_{xx} &= \frac{E(1-\nu)}{(1+\nu)(1-2\nu)}\varepsilon_{xx} + \frac{E\nu}{(1+\nu)(1-2\nu)}\varepsilon_{yy} \\
\sigma_{yy} &= \frac{E\nu}{(1+\nu)(1-2\nu)}\varepsilon_{xx} + \frac{E(1-\nu)}{(1+\nu)(1-2\nu)}\varepsilon_{yy} \\
\tau_{xy} &= \frac{E}{2(1+\nu)}\gamma_{xy}
\end{aligned} \tag{27}$$

thus comparison with Equations (26) gives the following equivalences:

$$\frac{E(1-\nu)}{(1+\nu)(1-2\nu)} \equiv \frac{\sqrt{3}}{4}(3k_n + k_s) \tag{28}$$

$$\frac{E}{2(1+\nu)} \equiv \frac{\sqrt{3}}{4}(k_n + k_s) \tag{29}$$

After some rearrangements, the relationship between the discrete element springs and the elastic properties of a plane strain continua are given by

$$k_n = \frac{E}{\sqrt{3}(1-2\nu)(1+\nu)} \tag{30}$$

$$k_s = \frac{E(1-4\nu)}{\sqrt{3}(1-2\nu)(1+\nu)} \tag{31}$$

Plane stress:

$$\begin{aligned} \sigma_{xx} &= \frac{E}{(1-\nu^2)}\varepsilon_{xx} + \frac{E\nu}{(1-\nu^2)}\varepsilon_{yy} \\ \sigma_{yy} &= \frac{E\nu}{(1-\nu^2)}\varepsilon_{xx} + \frac{E}{(1-\nu^2)}\varepsilon_{yy} \\ \tau_{xy} &= \frac{E}{2(1+\nu)}\gamma_{xy} \end{aligned} \tag{32}$$

After some rearrangements, the relationship between the discrete element springs and the elastic properties of a plane stress continua are given by

$$\frac{E}{(1-\nu^2)} \equiv \frac{\sqrt{3}}{4}(3k_n + k_s) \tag{33}$$

$$\frac{E}{2(1+\nu)} \equiv \frac{\sqrt{3}}{4}(k_n + k_s) \tag{34}$$

hence

$$k_n = \frac{E}{\sqrt{3}(1-\nu)} \tag{35}$$

$$k_s = \frac{E(1-3\nu)}{\sqrt{3}(1-\nu^2)} \tag{36}$$

These expressions were first described by Morikawa *et al.* [8] and developed further by Mustoe and Griffiths [11].

It is interesting to note that the equilateral element arrangement used in this formulation limits the value of Poisson's ratio ν to a maximum of 1/4 in plane strain from Equation (31), and a maximum of 1/3 in plane stress from Equation (36) corresponding to a shear spring stiffness of zero. This observation in the case of plane stress was also noted by Hrennikoff [1] for members 'devoid of any flexural rigidity'.

VALIDATION EXAMPLES

In this section the equivalences described by Equations (30), (31), (35) and (36) are validated by comparison with solid 2-D elasticity solutions. In each case, the discrete element results are compared with analytical solutions from classical elasticity and/or finite element solutions using solid finite elements. The implementation of the discrete element formulation described above is achieved by substitution of the element stiffness matrix given by Equation (13) into a standard beam-column structural analysis program such as that described by Smith and Griffiths [12]. An automatic mesh generation code was created as a pre-processor to the main program to generate equilateral arrangements of elements oriented in a similar pattern to that shown in Figure 7.

Uniform axial compression (plane strain)

In this example a mesh of width $W = 17$ and height $H = 17.32$ units was subjected to a uniform axial compressive stress of $\sigma_y = 1$ unit. As shown in Figure 8, the boundary conditions constrain the mesh to remain rectangular as it deforms. The forces were applied to the top surface of the mesh in the ratio:

$$\tfrac{1}{2} : 1 : 1 : \ldots : 1 : \tfrac{1}{2}$$

For different values of the spring constants k_n and k_s, axial and lateral deformations, δ_y and δ_x, respectively, were computed using the finite element program. From elastic theory (Equations (27)), the properties E and ν that would have resulted in those deformations in plane strain are given by

$$E = \sigma_y(1 - \nu^2)\frac{H}{\delta_y} \tag{37}$$

$$\nu = \frac{-H/W}{\delta_y/\delta_x - H/W} \tag{38}$$

By comparison, the properties E and ν implied by the equivalent discrete element theory in plane strain are given by rearrangement of Equations (30) and (31) as follows:

$$E = \frac{\sqrt{3}k_n}{8}\left(5 - \frac{k_s}{k_n}\right)\left(1 + \frac{k_s}{k_n}\right) \tag{39}$$

$$\nu = \frac{1}{4}\left(1 - \frac{k_s}{k_n}\right) \tag{40}$$

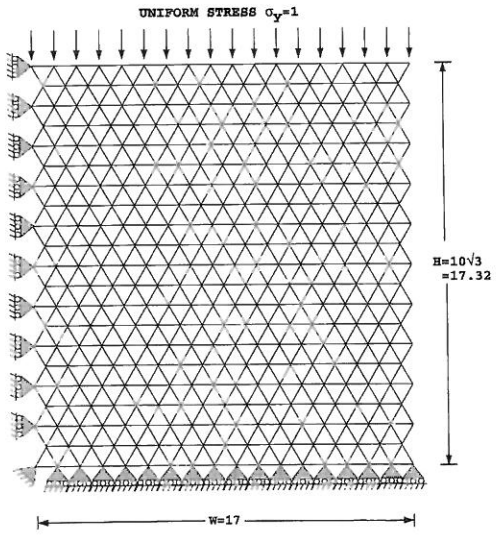

Figure 8. Axial compression of a block of elastic material in plane strain.

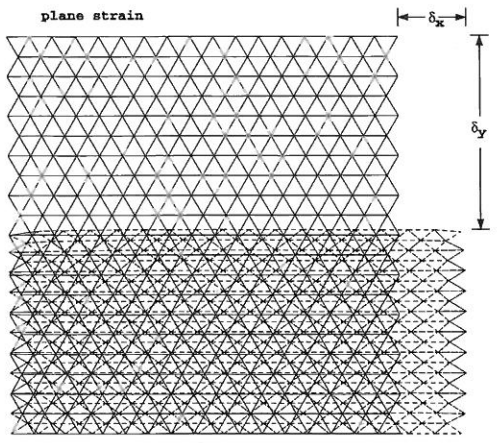

Figure 9. A typical deformed mesh under uniform axial loading in plane strain.

Table I. Results from axial compression analyses (plane strain).

Spring stiffness		Computed displacement		Continuum elastic Equations (37) and (38)		Equivalent elastic Equations (39) and (40)	
k_n	k_s	δ_y	δ_x	E	ν	E	ν
1	1	−10.01	0.00	1.723	0	1.723	0
1	0.5	−11.67	1.69	1.460	0.13	1.461	0.125
1	0.001	−15.01	5.17	1.076	0.26	1.083	0.25

A typical deformed mesh with the displacements magnified for clarity is shown in Figure 9 and the results summarized in Table I.

The table shows excellent agreement between the computed and theoretical elastic constants.

Self-weight loading (plane strain)

In this example, the same mesh considered in Figure 8 is subjected to self-weight loading. This implies a vertical (negative) force proportional to the amount of material 'attached' to each node. The different types of nodes are clearly shown in Figure 7. The majority of nodes are internal (type E), and connect six surrounding elements, each contributing one-third of its area. These internal nodes identify with an area equal to twice the area of each equilateral triangle as discussed previously. Other boundary nodes could connect one (type A), two (type B), three (type C) or four (type D) equilaterals, each contributing one third of its area. Thus type A gets one-third, type B gets two-thirds, and so on.

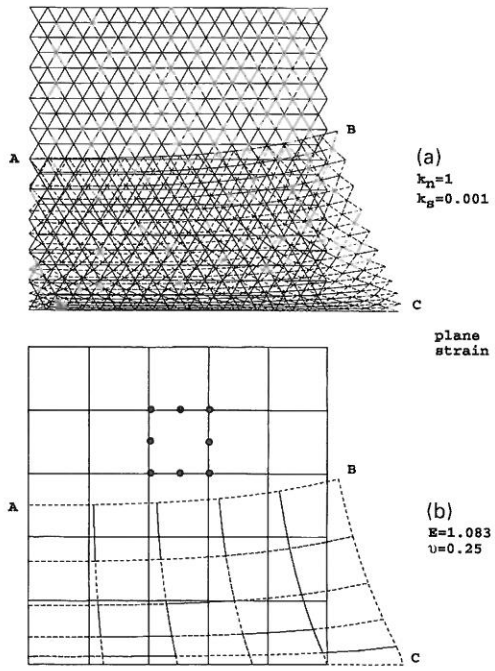

Figure 10. Deformed element due to self-weight loading in plane strain: (a) discrete elements; (b) solid elements. Unit weight, $\gamma = 1.0$.

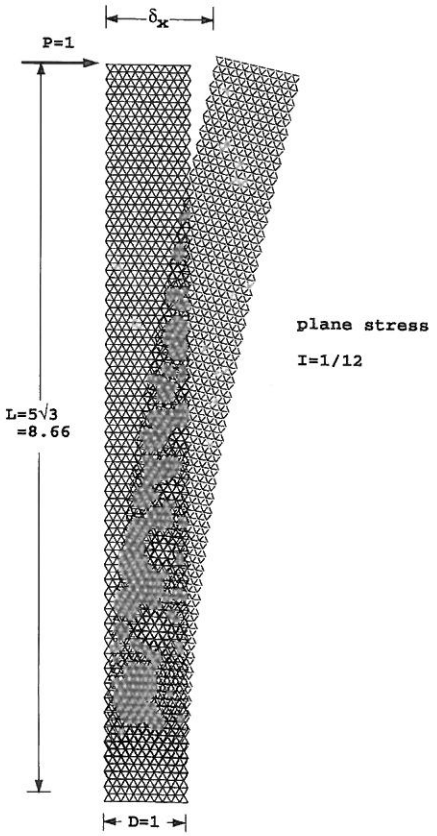

Figure 11. Cantilever in plane stress subjected to a unit transverse tip load.

The deformed mesh assuming a unit weight of unity is shown in Figure 10, together with the same problem analysed using solid eight-node quadrilateral elements. Both figures are scaled such that the vertical deformation at point A appears as half the initial height of the element. The actual deformations computed by both analyses at each corner of the block for different combinations of k_n and k_s (and hence E and v from Equations (39) and (40)) are shown in Tables II and III.

The tables indicate excellent agreement between the displacements at A, B and C computed by the two methods. The slight loss of symmetry in the case where $k_n = k_s = 1$ is thought to be due to numerical rounding errors in the single precision calculations.

A cantilever supporting a point load at its tip (plane stress)

As a more severe test, this example examines the ability of the discrete element model to reproduce bending effects. The cantilever shown in Figure 11 is subjected to a unit transverse point load $P = 1$ at its tip under plane stress conditions.

Table II. Results from discrete element self-weight analyses (plane strain).

Spring stiffness		A		B	C
k_n	k_s	δ_y	δ_x	δ_y	δ_x
1	1	−84	−2	−83	2
1	0.5	−100	2	−91	22
1	0.001	−134	9	−108	66

Table III. Results from solid 8-node element self-weight analyses (plane strain).

Equivalent elastic		A		B	C
E	v	δ_y	δ_x	δ_y	δ_x
1.723	0	−87	0	−87	0
1.461	0.125	−103	3	−95	23
1.083	0.25	−136	10	−113	67

The properties E and v implied by the equivalent discrete element theory in plane stress are given by rearrangement of Equations (35) and (36) as follows:

$$E = 2\sqrt{3}k_n \left\{ \frac{1 + k_s/k_n}{3 + k_s/k_n} \right\} \tag{41}$$

$$v = \frac{1 - k_s/k_n}{3 + k_s/k_n} \tag{42}$$

The 'slender beam' solution for the tip deflection of a cantilever is given by

$$\delta_x = \frac{PL^3}{3EI} \tag{43}$$

where P is the tip load and I is the (constant) second moment of area of the section. The cantilever shown in Figure 11 however, has a non-uniform section due to the equilateral triangles used in its discretization. While a direct comparison with Equation (43) cannot be made, an approximate comparison is possible using a beam length $L = 5\sqrt{3}$, and an *average* section width of 0.95 ($I = 0.95^3/12$). In this case the 'slender beam' solution from Equation (43) gives $\delta_x \approx 3030/E$. This approximate 'slender beam' solution for the tip deflection using E from Equation (41) is then compared with the computed value of δ_x using the discrete element approach with different combinations of k_n and k_s in Table IV. The agreement is reasonable, with the discrete element results giving a tip displacement that is between 10 per cent and 15 per cent too stiff.

Deflection under a flexible strip footing (plane strain)

The final example shown in Figure 12 considers the settlement of a strip footing subjected to a unit distributed load and supported by an elastic layer of finite thickness. In order to facilitate comparison with published solutions to this problem by Poulos and Davis [13], a footing of total

Table IV. Results from cantilever analyses (plane stress).

Spring stiffness		Computed displacement	Equivalent elastic Equations (41) and (42)		Slender beam theory Equation (43)
k_n	k_s	δ_x	E	v	δ_x
1	1	1518	1.732	0.0	1750
1	0.5	1779	1.485	0.143	2041
1	0.001	2381	1.155	0.333	2624

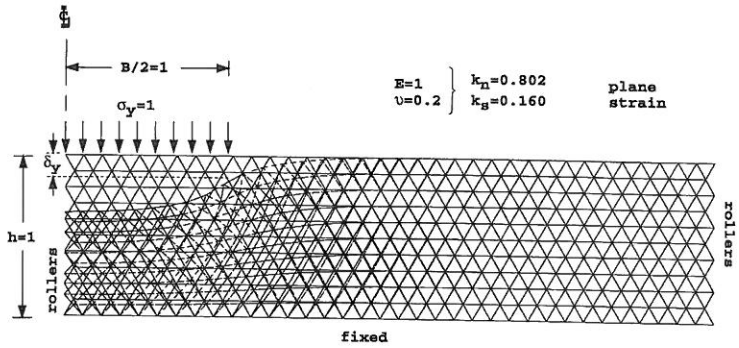

Figure 12. Flexible footing on a finite elastic layer under plane strain conditions.

width $B=2$ was selected together with elastic properties $E=1$ and $v=0.2$. By taking account of symmetry with rollers down the left side of the mesh, only one half of the footing is modeled.

In order to reproduce the required elastic properties in plane strain, the discrete element spring stiffness values were computed from Equations (30) and (31) to be $k_n=0.802$ and $k_s=0.160$.

The computed settlement beneath the edge of the footing was $\delta_y=0.45$ which compares well with the Poulos and Davis result (p. 103, Figure 5.2) of $\delta_y=0.43$.

CONCLUDING REMARKS

The theory and validations described in the paper have confirmed that a 2-D elastic continuum can be modelled using a grillage of beam-like finite elements based on discrete element concepts. Both plane strain and plane stress examples were presented and good agreement obtained between displacements obtained from the discrete element formulation and analytical and/or solid finite element solutions.

An interesting observation was that there was an upper limit on the magnitude of Poisson's ratio that could be reproduced by the method with 0.25 being the maximum for plane strain and 0.33 the maximum for plane stress. It is possible that other arrangements of discrete elements might lead to less restrictive values; an obvious choice being a loose-packed discrete element assembly leading to a square arrangement of 'beam' elements. The equivalent beam element stiffness matrix described in this paper opens up the possibility of many different arrangements, including random assemblies of different sized 'particles'. All the different arrangements will presumably lead to a different

relationship with solid elasticity. A natural extension of the current methodology currently under investigation by the authors is to develop the three-dimensional relationships between discrete and continuum elasticity. Although stresses can be calculated in the current method via the derivative of the strain energy density function, the paper has concentrated on the calculation of displacements. The subject of stress analysis requires further investigation, however in extending the method to the analysis of fracture, some form of failure criterion will need to be introduced. Whether this will be based on a limiting stress value (e.g. von Mises) or in limiting the magnitude of the normal and shear spring forces is currently a topic of investigation. Once this is resolved, it is envisaged that the introduction of fracture or failure of the discrete element assembly would follow an iterative algorithm, not unlike the non-linear procedures described in Smith and Griffiths [12] for modelling plastic hinge development and, ultimately, collapse of framed structures.

APPENDIX: NOTATION

B	width of footing
c	$\cos\theta$
D	depth of cantilever
E	Young's modulus
f_i/f_i'	term in global/local element 'force' vector
H	height of block
I	second moment of area
k_i/k_i'	term in global/local element stiffness matrix
k_n	normal spring
k_s	shear spring
L	length of cantilever
P	load applied to cantilever tip
r	discrete element radius
s	$\sin\theta$
u_i/u_i'	term in global/local element 'displacement' vector
v	'volume' of equilateral zone
V_o	strain energy density
W	width of block
W	strain energy stored in a single element
W_{tot}	strain energy stored in an equilateral zone
x, y	global Cartesian co-ordinates
x', y'	local Cartesian co-ordinates
β	average element nodal rotation
γ_{xy}	engineer's shear strain
δ_x	displacement in the x-direction
δ_y	displacement in the y-direction
ε_0	local element axial strain
ε_{xx}, ε_{yy}, ε_{xy}, ε_{yx}	strain tensor terms

θ element angle to horizontal

σ_{xx}, σ_{yy}, σ_{xy}, σ_{yx} stress tensor terms

σ_y stress applied in the y-direction

τ_{xy} shear stress

ψ_θ local element rotation

$\mathbf{f}/\mathbf{f}'$ element global/local 'force' vector

$\mathbf{k}/\mathbf{k}'$ element global/local stiffness matrix

$\mathbf{k}_{ij}$ partition matrix of $\mathbf{k}'$

$\mathbf{u}/\mathbf{u}'$ element global/local 'displacement' vector

$\mathbf{t}$ transformation matrix

ACKNOWLEDGEMENTS

The writers acknowledge the support of NSF grant numbers CMS-9713442 and GER-9554559.

REFERENCES

1. Hrennikoff A. Solution of problems of elasticity by the framework method. *Journal of Applied Mechanics* 1941; A169–A175.
2. Sridhar N, Yang W, Srolovitz DJ. Microstructural mechanics-model of anisotropic-thermal-expansion-induced microcracking. *Journal of the American Ceramic Society* 1994; **5**:1123–1138.
3. van Mier JGM, Vervuurt A, Schlangen E. Boundary and size effects in uniaxial tensile tests: a numerical and experimental study. In *Fracture and Damage in Quasibrittle Structures*, Chapter 25. Bazant ZP *et al.* (ed.), E and FN Spon, 1994; 289.
4. Kawai T. New element models in discrete structural analysis. *Japan Society of Naval Architects* 1977; **141**:174.
5. Kawai T, Kawabata KY, Kondou I, Kumagai K. A new discrete model for analysis of solid mechanics problems. In *Proceedings of the 1st Conference on Numerical Methods and Fracture Mechanics*, Swansea, 1978.
6. Hocking G, Mustoe GGW, Williams JR. Validation of the CICE discrete element code for ice ride-up and ice ridge cone interaction. In *ASCE Specialty Conference*, "*ARCTIC* '85", San Francisco, 1985.
7. Mustoe GGW. A generalized formulation of the discrete element method. *Engineering Computations* 1992; **9**(2): 181–190.
8. Morikawa H, Sawamota Y, Kobayashi N. Local fracture analysis of a reinforced concrete slab by the discrete element method. In *Proceedings of the 2nd International Discrete Element Methods*. MIT Press: Cambridge, MA, 1993.
9. Matsuoka O, Kato S, Koide H. Continuum mechanics of shell structures composed of grid works. *Transactions of the Archaeological Institute of Japan* 1971; **184**:63–71 (in Japanese).
10. Timoshenko SP, Goodier JN. *Theory of Elasticity* (International Edition). McGraw-Hill: New York, 1982.
11. Mustoe GGW, Griffiths DV. An equivalent continuum model using the discrete element method. *Proceedings of the 12th ASCE Engineering Mechanics Conference*, 1998; 989–992.
12. Smith IM, Griffiths DV. *Programming the Finite Element Method* (3rd edn). Wiley: Chichester, 1998.
13. Poulos HG, Davis EH. *Elastic Solutions for Soil and Rock Mechanics*. Wiley: Chichester, 1974.

Exploiting the use of simulation and visualization in your product philosophy

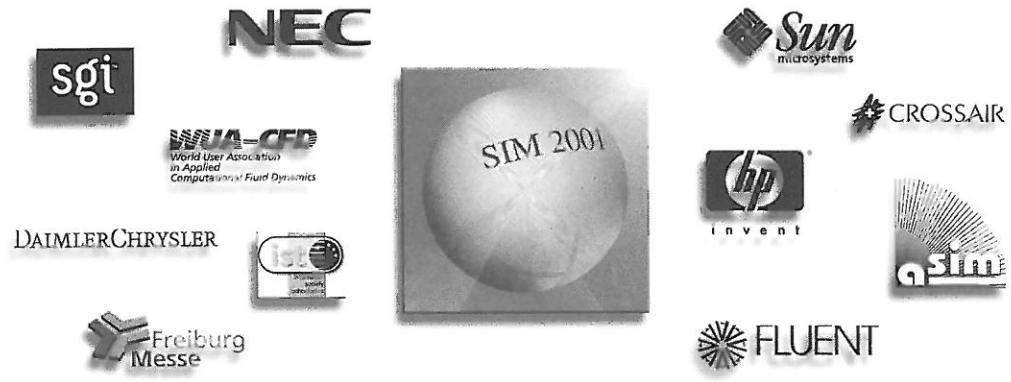

SIM 2001®, June 17 to 21, 2001 in Freiburg im Breisgau, Germany

The SIM 2001 Trade Fair is the international knowledge exchange in applied simulation and visualization, showing most available hard- and software and industrial applications in many fields.

The SIM 2001 Conferences are held at the same time alongside. • Strategic importance of simulation and visualization for industry in the next decade (Official SIM-Overview-Conference in cooperation with Exhibitors and European Universities) • 5th World Conference in Applied Fluid Dynamics (L&A GmbH, Basel with WUA-CFD, Basel, Switzerland).

The SIM 2001-Recruiting Day is planned to be the international meeting point for professional engineers in simulation and visualization in order to meet leading employers from industry and vice versa.

The SIM 2001-Partnering Day invites all visitors and exhibitors to come together for potential cooperations and projects, to discuss guidelines for the future development and to seek for possible partnerships.

The SIM 2001-Exhibitors will be the vendors of most related hard- and software and a large number of industrial companies who present their services, applications and significant results.

The SIM 2001-Visitors are responsibles for product development, engineers, application oriented scientists, development leaders and heads of technology management.

The Organizers of SIM 2001 are Löffler & Associates GmbH, Basel, Switzerland (info@sim2001.com) in cooperation with Messe Freiburg, Germany, (info@messe-freiburg.de).

The Sponsors of SIM 2001 are • NEC • HP • SGI • SUN Microsystems • DaimlerChrysler • Fluent • Crossair • ASIM and other exhibitors.

The Cooperators of SIM 2001 are • Löffler & Associates GmbH, Basel, CH • Messe Freiburg, Freiburg i. Br., D • World User Association in Applied Computational Fluid Dynamics (WUA-CFD), Basel, CH • International Association for Vehicle Design (IAVD), Geneva, CH.

For further Information please call us +41 61 695 93 95 or fax us +41 61 695 93 90 or go on our web site under www.sim2001.com